Surface Functionalization of Thermoset Composite for Infrared Hybrid Welding

Henri PERRIN (henri.perrin@list.lu)
Material Research and Technology Department, Luxembourg Institute of Science and Technology, 5 rue Bommel, Hautcharage, 4940, Luxembourg https://orcid.org/0000-0002-3643-9299

Grégory Mertz
Luxembourg Institute of Science and Technology

Noha-Lys Senoussaoui
Luxembourg Institute of Science and Technology

Loïc Borghini
Luxembourg Institute of Science and Technology

Sébastien Klein
Luxembourg Institute of Science and Technology

Régis Vaudemont
Luxembourg Institute of Science and Technology

Research

Keywords: infrared welding, thermoset composite, thermoplastic composite, dissimilar joining

Posted Date: October 20th, 2020

DOI: https://doi.org/10.21203/rs.3.rs-93089/v1

Version of Record: A version of this preprint was published at Functional Composite Materials on April 6th, 2021. See the published version at https://doi.org/10.1186/s42252-021-00021-5.

Abstract

Fusion assembly is a highly promising technique to join thermoplas- tic to thermoset composites, enabling the use of both the most affordable com- posite material and process for each sub structure.Yet, some major challenges need to be pull through such as the functionalizing of the thermoset compos- ite surface by co-curing an appropriate thermoplastic interlayer or realizing a fast and robust welding process that fulfils all quality and mechanical require- ments. In the present paper, we investigated the potential of Polyetherether- ketone (PEEK) and its amorphous (PEEK A) and semi-cristalline (PEEK SC) states as interlayer materials, co-cured onto the thermoset composite. A surface preparation by atmospheric plasma process demonstrated that both PEEK state materials can be used as interlayer with auspicious resulting ad- hesion properties. The influence of the plasma treatment on surface properties and morphology is also experimentally characterized. An infrared (IR) welding process, barely studied in the literature, is studied to assemble hybrid struc- tural composite. In order to avoid the expected thermal degradation of the thermoset matrix, a dissimilar infrared heating input power is proposed. More- over, to decrease the possible thermal degradation of the thermoset composites during the fusion bonding, a dissimilar infrared welding process have been ex- plored. Single lap shear test and failure mode analysis have been performed to highlight the promising performance of PEI as well as PEEK interlayer based hybrid joint.

Introduction

Aeronautics have to address two main challenges in the upcoming decade: the expected production growth and the cost reduction of composite manufac- turing, assembly and control Gardiner (2018) . Indeed, composite materials are a realistic alternative and a key component to reduce both the weight and CO_2 emissions without affecting the mechanical performance. Compos- ites used to replace metallic part are composed of a reinforcement generally glass or carbon fibres and a polymeric matrix, being either a thermoset or a thermoplastic. The use of thermoset over thermoplastic is depending on the application, properties and cost. For example, in the case of aerospace indus- try thermoset based composites (TSC) are currently being used because of their good compression, fatigue and creep resistance as well as their econom- ical production to large parts. Currently, TSC are mainly assembled by time and labour consuming bonding/riveting techniques. Inversely, thermoplastic based composites (TPC) demonstrate high ductility, fracture toughness, im- pact resistance and can be quickly manufactured by stamping and joined to other TPC by welding.

In order to produce materials in a more efficient and affordable way, the combination of thermoset and thermoplastic composites defined here as “hy- brid” composites open new doors and potential scopes. Indeed, hybrid com- posites will enable the use of the right material and the right manufacturing process for the right substructure. However, two main challenges need to be dealt with. First, cured thermoset composites cannot be melted at tempera- tures necessary to weld high performance thermoplastic. Second, the thermal degradation of thermoset composites during fusion process have to be avoided or at least minimized.

In the literature, many authors explore the use of Polyetherimide (PEI) as an interface material for hybrid welding. PEI has been demonstrated as a good candidate to act as an interfacial layer towards the thermoset composite. PEI is generally preferred due to its intrinsic miscibility with epoxy resin, which leads to high resulting adhesion properties. However, this advantage also represents a weak point regarding in-service applications. PEI polymer presents a limited withstand to aeronautics fluids. Still, there is another challenge to overcome

after co-curing: to join the co-cured TSC bearing a thermoplastic –rich layer with the other part efficiently and in a short time. Therefore, the welding process needs to provide a concentrated heat in a limited time. Today three main technologies exist to weld composites such as resistance Xiong et al. (2019) , induction, ultrasonic welding da Costa et al. (2012) Tsiangou et al. (2020) . Regarding the different solutions proposed to join materials by welding Infrared (IR) welding possesses numerous advantages such as an ability quickly to heat (typically around 2-25 seconds), a capacity to attenuate contamination risks, thus allowing high productivity rates of reproducible joints in automated systems for thermoplastic materials as stated by da Costa et al. (2012). As far as we know, IR welding has barely been discussed and investigated to join hybrid high performance composites. IR welding of structural thermoplastic composite have been investigated by Allaer et al. (2012) .

In the present work, a new approach of hybrid thermoset/thermoplastic composite is proposed by welding both composites by an automated fast infrared technology. We propose an original approach paving the way for a more global composite structure cost reduction by hybrid material design and assembly through i) the in-process functionalization of thermoset composite bringing weldability properties, ii) the welding by infrared welding enabling dissimilar welding.

Experimental Procedures

2.1 Materials for welding

2.1.1 *Thermoplastic composite*

In this work, carbon fiber reinforced PEEK consolidated laminate supplied by Toray Advanced Composites has been selected. The 1.86mm thick laminate is made of 6 plies of 5H satin weave from 3K T300 carbon fiber roving with a quasi- isotropic lay-up.

2.1.2 Interlayer surface preparation

Two reference of 25 μm PEEK film have been chosen at an amorphous (PEEK A) and semi-cristalline (PEEK SC) state (Aptiv®2000 from Victrex®) with a matte/gloss finishing. A 50 μm PEI (ULTEM *T M* from Sabic) film is also included in this study as reference DSC analysis presented on Figure 1 shows that PEEK A presents a low level of cristallinity, 8% as received, compared to the 34,7 % of cristallinity of PEEK SC as received. PEEK A start to recrystallize by heating up to 160◦C. Per convention, the matte surface of the films is in contact with the TSC, and the gloss one is welded on the TPC.

Cleaning up and activation steps were performed using an atmospheric pressure Dielectric Barrier Discharge (DBD) reactor. Briefly, plasma was ignited in a DBD (3 mm gap between the electrodes) in which each of the two high voltage aluminum plate electrodes is protected by a 3.25 mm thick glass plate. Plasma discharge was generated by an AC power supply set at 450W and 6 kHz, with a flow of 80% N_2 and 20% O_2 . The top electrode moved over the bottom one at a constant 4 m.min −1 speed in a to and fro movement. The deposition time was set to 1 minute.

Through the proposed surface treatment by N_2/O_2(80/20) atmospheric plasma Kuzminova et al. (2014) , the wettability of the three interlayer films is improved through a cleaning and chemical activation. In order to better understand the time contribution of the treated surface, three post-treatment time are selected for this study: 1 minute, 3 days and 7 days after treatment. An interlayer film without treatment of each interlayer materials is also included in the present work.

It is well-known in the literature Fricke et al. (2012) that plasma treatment can affect significantly the surface roughness of the polymer substrate. In or- der to quantify the expected surface roughness modification, 3D profilometry measurements have been performed on both non-treated and plasma-treated interlayer films. Due to the initial roughness of the selected layer, profilometry have been preferred over Atomic Force microscopy (AFM). The used pro- filometer is a KAR TENCOR P17 and a scanning area of 50 μm per 50 μm have been selected.

Plasma treatment is also industrially used to activate the polymer surface and consequently increase their wettability. Wettability measurements have been done by a contact angle system OCA 15 from Dataphysics. A series of 5 sessile water droplets of 2 μL were deposited on the surface of each sample by means of a syringe pump. The contact angle value has been extracted from the droplet shape by using a numerical fit based on the Laplace-Young model. Plasma treatment is also responsible for major surface chemical changes. X- ray photoelectron spectroscopy (XPS) was performed to track chemical surface modifications with a VG SCIENTA SES-2002 spectrometer equipped with a concentric hemispherical analyzer. The incident radiation used was generated by a monochromatic Al Kα x-ray source (1486.6 eV) operating at 420W (14 kV; 30 mA). Photo-emitted electrons were collected at a take-off angle of 90◦ from the surface substrate, with electron detection in the constant analyzer energy mode (FAT). Wide scan spectrum (survey) signal was recorded with a pass energy of 500 eV and for high resolution spectra (C1s and O1s) pass energy was set to 100 eV. The analyzed surface area was approximately 24mm2 and the base pressure in the analysis chamber during the experiment was about 10 −9 mbar. The spectrometer energy scale was calibrated using the Ag 3d5⁄2, Au 4f7⁄2 and Cu 2p3⁄2 core level peaks, set respectively at binding energies of 368.2, 84.0, and 932.6 eV. Spectra were subjected to a Shirley background and peak fitting was made with mixed Gaussian-Lorentzian components with equal full-width-at-half maximum (FWHM) using CASAXPS version 2.3.18 software. The surface composition, expressed in atom%, was determined using integrated peak areas of each components and took into account transmission factor of the spectrometer, mean free path and Scofield sensitivity factors of each atom. All the binding energies (BE) were referenced to the C1s peak at 285.0 eV and given with a precision of 0.1 eV. The O/C and N/C ratio have been obtained by using the value from the surface composition analysis.

2.1.3 Functionalized thermoset composite by Liquid Resin Infusion (LRI)

Liquid Resin Infusion (LRI) process are used to co-cure the thermoplastic interlayer onto the TSC surface. The interlayer is first placed on the molding tool surface. Dry carbon fibers reinforcement, made of 6 plies of carbon fabric layup at 0◦, supplied by Hexcel with following type of yarns: warp, HexTow AS4C GP 3K; weft : HexTow AS4C GP 3K . The fabric's weave style is twill 2/2 for a nominal weight 200 g/m2. One 600x 600 mm composite plate is injected per interlayer treatment conditions. All three interlayer material , 200 mm x 600mm will be integrated on each plate.

Onto the dry carbon fiber reinforcement a peel ply, resin distribution media and a vacuum bag complete the set-up. The latter is place in a 2 m3 oven from SAT Thermique, +/-5 ◦C accurate at 410◦C. An ISOJET injection machine composed of a pressured heated tank of 25L, a resin flow rate control system and a heated transfer pipe, fully controlled automatically through a Schneider Citect/SQL monitoring automate.

The selected thermoset resin is the RTM6-2, bi-component supplied by Hexcel. The cure cycle has been adapted in order to launch the resin poly- merisation above the PEEK T_g and below the recrysatlisation temperature of the PEEK A. This cycle should promote the Interlayer/TSC interface by molecule diffusion Shi et al. (2017) . The thermal cycle of 2h at 150◦C + 2h @ 180◦C with 5◦C heating ramp rate have been selected. The applied receipt is described in Table 1 .

On Figure 2 the functionalized TSC surface is shown after demoulding. It should be noted, that the non-treated PEEK SC configuration present no adhesion after demoulding and consequently, which is why no welding tests are possible. Plates are water jet cut to a size 100 mm x 170 mm for be then welded in the next stage.

2.2 Infrared welding process for dissimilar join

2.2.1 IR Welding principle

IR welding experiment were carried out using FRIMO's Infrared-Welding Machine ECO800 equipped with a welding tool enabling the assembly of two 100 mm length composite plates with an overlap of 12.7 mm. Welding line is 170 mm width. Single lap shear samples are cut in a later stage through water jet cutting at width of 25mm.

The welding tool is composed of an upper and lower moulds (Cf. Figure 3) where the plates are positioned through vacuum gripper. Both moulds are fixed on mobile table enabling the definition at each process step of they position in vertical direction. A mobile heating frame able to move along the horizontal direction. On both side of the heating frame are fixed a set of infrared lamps. Each lamp is control individually enabling a control of the power as function of the time. By dissimilar material welding, the cycle time of the upper and the lower set of IR lamp are adapted to the thermal profile required by each material melting behavior.

2.2.2 IR welding process for dissimilar material welding

For dissimilar welding, the principle (Cf. Figure 4) consists to heat up each surface to assemble though an appropriate thermal cycle by controlling individually short wave infrared emitters, on the thermoset composite side and the thermoplastic composite side. Our approach consist to heat up the thermoplastic composite up to the decompaction of around half of the material initial thickness, and heat up just before the end of the cycle the thermoset composite side as quick as possible, enabling the fusion of the thermoplastic film without permanent major degradation of the thermoset composite substrate. In this work, two different heating cycle time have been proposed: 27 seconds at 90% of the maximum infrared lamp power for the TPC, and 17 seconds for the TSC. The TSC heating cycle starts after 10 s delay compared to the TPC heating cycle start.

Figure 5 shows the thermal profile of both the welded surface and back surface of the TPC and TSC. Type K Thermocouples, with a 0.25mm diameters, have been positioned on the surface to weld of each welding partners, as well as between the welding partner and the tool. A SEFRAM DAS 240 data logger have been used for temperature acquisition with a sampling rate of 20 ms.

2.2.3 Thermal degradation of the TS matrix

Prior to the welding of TSC with TPC a more in depth study of the effect IR light towards the resin alone need to be investigated as such material is sensitive to high energy light or temperature which cause severe degradation and damage. The modification during the IR treatment was tracked by FTIR in reflection mode to assess the chemical variation. FTIR spectrum was performed on the surface of the as manufactured resin at different IR radiation time from 1 to 15s. From the spectrum we can noticed an increase of the peaks at 1660 cm −1 and the apparition of a shoulder at 1735 cm −1 which is related to the formation of carbonyls groups linked to the thermal degradation when the sample are subjected to the IR radiation in presence of oxygen Doblies et al. (2019) Villegas and Rubio (2015) . Moreover, a decrease of the bond at 1050 cm −1 with the time of irradiation increase which can be attributed to the epoxy backbone ether bridge. Such decrease can be assigned to chain scission and argue for the degradation/decomposition of the resin under the IR light. By using high energy IR irradiation modify the surface of the resin by a thermal degradation mechanism where oxidation and chain scission occur. Such observation can explain the failure observed in the next section where the failure occurs in the thermoset composite. For a future application the control of the power of IR lamp will be optimized to avoid the degradation but just applied enough energy to weld the material.

Results And Discussion

3.1 Surface functionalisation of TS composites

3.1.1 Interlayer roughness

Figure 7 shows that the effect of plasma treatment on surface roughness is significant. The root mean square value (Sq) is similar before and after plasma treatment, respectively 0.0213 μm and 0.0209 μm. Contrariwise, the Kurtosis value (Sku) describing the sharpness of the roughness profile is strongly

different. In case of non-treated PEEK SC, Sku is 7.25, characteristics of a spiked height distribution. For plasma treated PEEK SC, Sku is much lower, about 2.73. Here the height distribution is skewed above the mean plane. By plasma treatment, the initial primary roughness of the PEEK SC as received is complemented by a secondary roughness. PEEK A and PEI presents a similar trend with a shift of the height distribution towards lower values.

3.1.2 *Interlayer wettability*

Prior to the IR welding the surface of the thermoset composites needs to be modify in order to avoid its thermal degradation when subjected to the IR lamp from the welding. To protect the TS composites, an interlayer of PEEK or PEI is introduced during the manufacturing, such interlayer will play another role, and will promote the interpenetration with the PEEK composites. To improve the compatibility of the interlayer with TS, the surface has been modified by plasma treatment. Such fast treatment Kuzminova et al. (2014) modifies the extreme surface by cleaning and chemical activating it, through the addition of radicals and polarity. Consequently, the done treatment will increase the compatibility with the resin, improve the inertness of the interlayer surface and will create strong chemical bond with the surface of the resin. Surface analysis of the interlayer have been performed prior and after treatment. WCA results are depicted in Figure 8 .

Before plasma treatment PEI, PEEK A and PEEK SC surfaces respectively highlight a WCA around 90 3◦,91 3◦ and 93 3◦. After plasma treatment, the WCA dropped significantly to 27 3, 33 3 and 34 3◦ respectively. After just 1 minute of oxidative plasma treatment the wettability of the interlayer surface noticeably drops; such changes in wettability can promote a better flow and adhesion of the thermoset resin during the TSC manufacturing by LRI.

3.1.3 *Chemical surface modification investigation by XPS*

To investigate deeper the chemical changes occurring at the surface of the interlayer XPS investigation have been performed and depicted in Figure 9 by following the O/C and N/C ratio. The O/C ratio increase from 0.18 to 0.31 and from 0.05 to 0.08 for PEI. The plasma treatment allowed to modify the surface by grafting some chemical functions based on oxygen and nitrogen needed to bond some materials, which are difficult to stick without surface modification- such as polyethylene for example. Here, the same approach is foreseen since the same trends are observed for PEEK A and PEEK SC. To conclude, by using plasma treatment- which is a fast and easy technique to implement and a dry process- the surface of the three interlayer have been modified. This could foster the interpenetration with the thermoset, and consequently increase the adhesion with the TS composites during the co-curing process.

3.1.4 *Analysis of the surface functionalized TS composites*

A pressure-controlled FEI Quanta FEG 200 scanning electron microscope (SEM) from FEI Company was used to get information about microstructure in the cross section of the samples. Samples were embedded in epoxy casting resin and subsequently grinded and polished until reach a scratch-free

surface is obtained.Figure 10 highlights the cross-section obtained by SEM of the samples bearing interlayer at their surface. Concerning the PEI interlayer, the thickness measured from micrographs have respectively decreased to 38 and 43 μm before and after plasma treatment, compared to the initial thickness of 50 μm. As previously discussed, the miscibility/compatibility between the resin and the PEI interlayer can explain the changes in the thickness measured by SEM. During the co-curing phase, the resin can, before its gelation point, interpenetrate and interdiffuse through the PEI interlayer and create a semi interpenetrating networks Vandi et al. (2012) Heitzmann et al. (2012) Gao et al. (2019) . However, no real difference can be observed and related to plasma treatment.

In contrary to PEI, the initial thickness of the PEEK A interlayer does not exhibit any change during co-curing since the same thickness of 25 μm is observed. Moreover, a clear and neat difference in the grey scale range from the micrograph occurred owing to the low miscibility between the resin and the PEEK interlayer. Although the plasma treatment does not demonstrate any improvement of the miscibility between the resin and the PEEK interlayer. The transition is neat without any voids arguing for a good adhesion, which probably occurs at the molecular or nanoscale and out of the capability of the SEM.

Concerning the interlayer without plasma treatment, no adhesion occurs: the PEEK interlayer can be easily separated by hand and no picture haas been depicted. In this case the semi-crystalline state does not allow the interpene- tration with the resin during the manufacturing process. Unexpectedly, after plasma treatment, the adhesion between the interlayer and the resin during the co-curing occurs and by SEM observation. Furthermore, no decohesion is visible between both components. The joint line seems smooth and without any defects. The initial thickness is effortless observed by SEM without any additional surface treatment, and even is so at the same order of magnitude compared to the initial thickness 25 μm. At the current state of our knowl- edge the plasma acts as a cleaner and as a surface activator that promotes the adhesion between the interlayer and the resin during the co-curing process, probably by creating a semi-interpenetrating network only at the extreme in- terlayer surface. A deeper investigation will be performed in a future paper to investigate more precisely the arising mechanism at the interface between both materials.

3.2 Welded dissimilar joint performances

3.2.1 Lap-shear test result

Figure 11 represents the obtained results from single lap shear mechanical tests performed on each sample. The value for untreated PEI is around 17.5 MPa and all treated samples are closer to 19 MPa. A slight increase occurs on the plasma-treated sample, which can not be directly explained y the surface treatment itself as failure occurs through the TSC instead at the interlayer interface. The same trends have been observed for amorphous and semi- crystalline PEEK a slightly higher value is reached after plasma treatment. Regarding the standard deviation of the lap shear test, this slight trend is considered as welding process uncertainties, and is’nt translating a direct effect of the plasma treatment waiting time after plasma treatment. Surprisingly, the waiting time after plasma treatment have no major impact on the resulting mechanical properties. Except for untreated PEEK SC where no adhesion happens with

the resin during co-curing. Resulting values of the mechanical performance of both PEEK are not so far from those of PEI, which mean that the IR welding process combined with appropriate surface activation is a powerful technique to strongly bond thermoset to thermoplastic composites.

3.2.2 Failure modeanalysis

In order to investigate the failure mode after the mechanical test, visual observation have been performed on test sample. Three type of failure mode have been observed: an adhesive failure at the TPC/interlayer interface, an adhesive failure at the interlayer/TSC interface and a cohesive failure through the TSC.

Figure 12 shows the failure surface of both welded partners using a PEEK A material as interlayer, without and with plasma treatment. It is interesting to notice that, without plasma treatment, the PEEK A interlayer present locally adhesive failure with the TSC. This failure mode is visible on two SLS samples of the five tested in this configuration. On this configuration, all three failure modes are observed. It is clear that plasma treatment plays a valuable role not only for PEEK SC material but also for PEEK A.

With plasma treatment, no more adhesive failure at the interlayer/TSC interface are observed. Failure mode are dominated by a failure through the TSC composite.

Figure 13 shows the failure mode for both PEEK SC and PEI in case of plasma treatment of the interlayer. Only cohesive failure through the TSC are observed. The same observation has been made for non-treated PEI post mortem analysis. The first ply of the TSC is still welded after the lap shear test.

Conclusions

1. A new approach to weld thermoset to thermoplastic composites is proposed in this paper by combining IR welding and interlayer surface preparation by plasma
2. Indeed, plasma technology was used to improve the adhesion of the surface of the Three induced effects of plasma have been asserted: the surface roughness alteration, the wettability increase, and the chemical surface modification. For PEEK SC, plasma treatment is mandatory in order to generate an adhesion by co-curing. For PEEK A, an improvement of the adhesion is distiguishable on the mechanical properties, and is confirmed later by the failure mode analyse. For PEI interlayer, no effect is observed as the welded joint failed through the TSC and not in the interlayer area.
3. The contribution of plasma treatment's three induced effects cannot clearly be established as failure mode occurs outside the interlayer The waiting time's variation after plasma treatment before co-curing is not a driven parameter. Surprisingly, even 7 days after the plasma treatment, mechanical properties are maintained at a similar level, which is an unexpected advantage for future indutrial exploitation.
4. Diffusion the TS matrix in the PEI interlayer was expected and have been observed through the reduction of the PEI thickness after co-curing. For both PEEK A and PEEK SC, no thickness variation have been observed but similar level of lap shear strength have been

5. Even through the obtained mechanical performance is under the indus- trial requirement, IR welding have been proved to be suitable to design hybrid composites without any additional element unlike resistive element and energy director for resistance and ultrasonic welding respectively, although the me- chanical performance are under the industrial requirement. Further research on the adhesion between the interlayer and the resin need to be done to better understand the underlying mechanisms as well as the optimization of IR weld- ing process parameters in order to avoid any TSC degradation, responsible for early stage

Declarations

Availability of data and materials

The datasets used and/or analyzed during the current study are available from the corresponding author on reasonable request

Funding

The project leading to this application has received funding from the Clean Sky 2 Joint Undertaking under the European Union's Horizon 2020 research and innovation programme under grant agreement No 831979. All authors gratefully thank the European Commission and the Clean sky II JU

Acknowledgments

The authors thank gratefully Yves Fleming for 3D-Profilometry measurement and Jerome Guillot, for XPS analysis.

Competing interest

The authors have no competing interest.

Author's contribution

Henri Perrin: conceived and design the by LRI in-process functionalization and IR welding experiments, analyzed and interpretated the data, wrote the paper, reviewed and edited the manuscript

Gregory Mertz: conveived, designed, perfomred and characterization sur- face treatment experiment , contributed writing the manuscript

Noha-Lys Senoussaoui: performed the thermal analysis experiments, con- tributed writing the manuscript

Loïc Borghini: performed the by LRI in-process functionalization experi- ments

Sébastien Klein: performed the IR welding experiments

Régis Vaudemont: conceived, design and performed the thermal analysis experiments, critically reviewed the manuscript

References

1. Allaer K, Baere ID, Paepegem WV, Degrieck J (2012) Infrared welding of car- bon fabric reinforced thermoplastics. JEC Composites Magazine 49(77):44– 47
2. da Costa AP, Botelho EC, Costa ML, Narita NE, Tarpani JR (2012) A review of welding technologies for thermoplastic composites in aerospace applications. Journal of Aerospace Technology and Management 4(3):255– 265, DOI 10.5028/jatm.2012.04033912
3. Doblies A, Boll B, Fiedler B (2019) Prediction of thermal exposure and mechanical behavior of epoxy resin using artificial neural networks and Fourier transform infrared spectroscopy. Polymers 11(2), DOI 10.3390/ POLYM11020363
4. Fricke K, Reuter S, Schroder D, von der Gathen VS, Weltmann KD, von Woedtke T (2012) Investigation of Surface Etching of Poly(Ether Ether Ketone) by Atmospheric-Pressure Plasmas. IEEE Transactions on Plasma Science 40(11):2900–2911, DOI 10.1109/TPS.2012.2212463
5. Gao X, Huang Z, Zhou H, Li D, Li Y, Wang Y (2019) Higher mechanical performances of CF/PEEK composite laminates via reducing interlayer porosity based on the affinity of functional s-PEEK. Polymer Composites 40(9):3749–3757, DOI 10.1002/pc.25236
6. Gardiner G (2018) Welding thermoplastic composites : CompositesWorld. Composite World pp 1–12
7. Heitzmann MT, Hou M, Veidt M, Vandi LJ, Paton R (2012) Morphology of an interface between Polyetherimide and epoxy prepreg. Advanced Ma-
8. terials Research 393-395(September):184–188, DOI 10.4028/www.scientific. net/AMR.393-395.184
9. Kuzminova A, Shelemin A, Kylián O, Choukourov A, Valentová H, Krakovský I, Nedbal J, Slavínská D, Biederman H (2014) Study of the effect of atmo- spheric pressure air dielectric barrier discharge on nylon 6,6 foils. Polymer Degradation and Stability 110:378–388, DOI 10.1016/j.polymdegradstab. 2014.10.001
10. Shi H, Sinke J, Benedictus R (2017) Surface modification of PEEK by UV irradiation for direct co-curing with carbon fibre reinforced epoxy prepregs. International Journal of Adhesion and Adhesives 73:51–57, DOI 10.1016/j.ijadhadh.2016.07.017
11. Tsiangou E, de Freitas ST, Villegas IF, Benedictus R (2020) Ultrasonic welding of epoxy- to polyetheretherketone- based composites: Investigation on the material of the energy director and the thickness of the coupling layer. Journal of Composite Materials 54(22):3081–3098, DOI 10.1177/ 0021998320910207

12. Vandi LJ, Hou M, Veidt M, Truss R, Heitzmann M, Paton R (2012) Interface diffusion and morphology of aerospace grade epoxy co-cured with thermo- plastic polymers. 28th Congress of the International Council of the Aero- nautical Sciences 2012, ICAS 2012 3(January 2012):1984–1992
13. Villegas IF, Rubio PV (2015) On avoiding thermal degradation during welding of high-performance thermoplastic composites to thermoset composites. Composites Part A: Applied Science and Manufacturing 77:172–180, DOI 10.1016/j.compositesa.2015.07.002
14. Xiong X, Zhao P, Ren R, Zhang Z, Cui X, Ji S (2019) Resistance welded composite joints strengthened by carbon fiber felt: Mechanical properties, failure modes and mechanism. Materials Research Express 6(8), DOI 10.1088/2053-1591/ab226b

Tables

Table 1 LRI main process parameters

Parameters	Value	Unit
Outgassing temperature	120	˚C
Outgassing vaccum level	1	mbar
Outgassing time	15	min
Injection mold temperature	120	˚C
Tank and tube temperature	120	˚C
Resin flow rate	50	g/min
Vaccum during injection	50	mbar
Injected mass	500	g

Figures

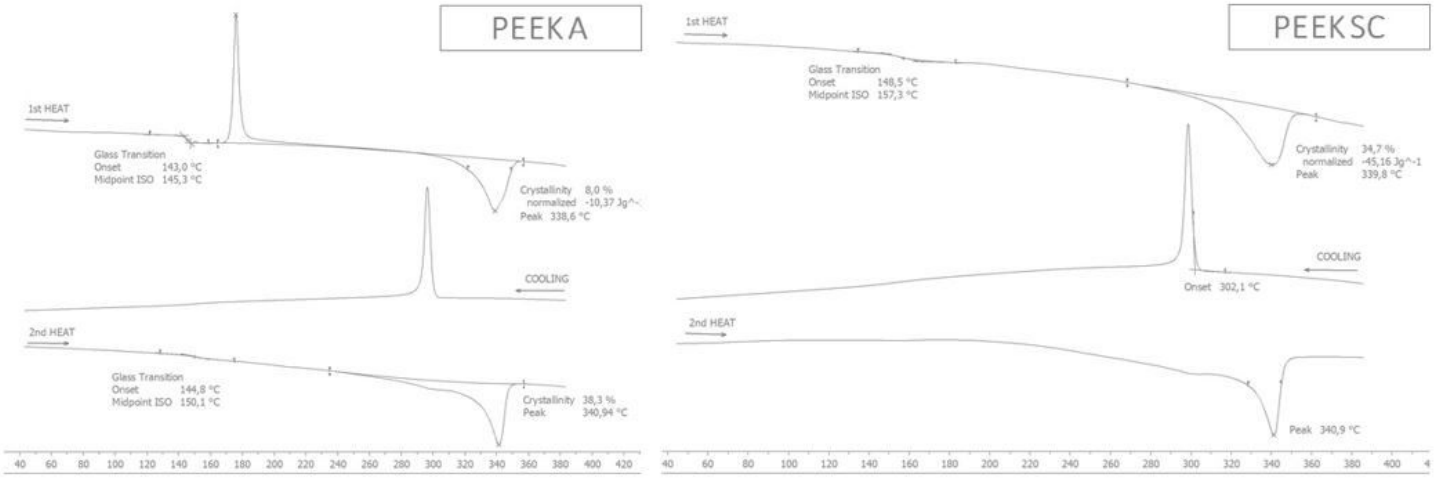

Figure 1

DSC of PEEK A and PEEK SC

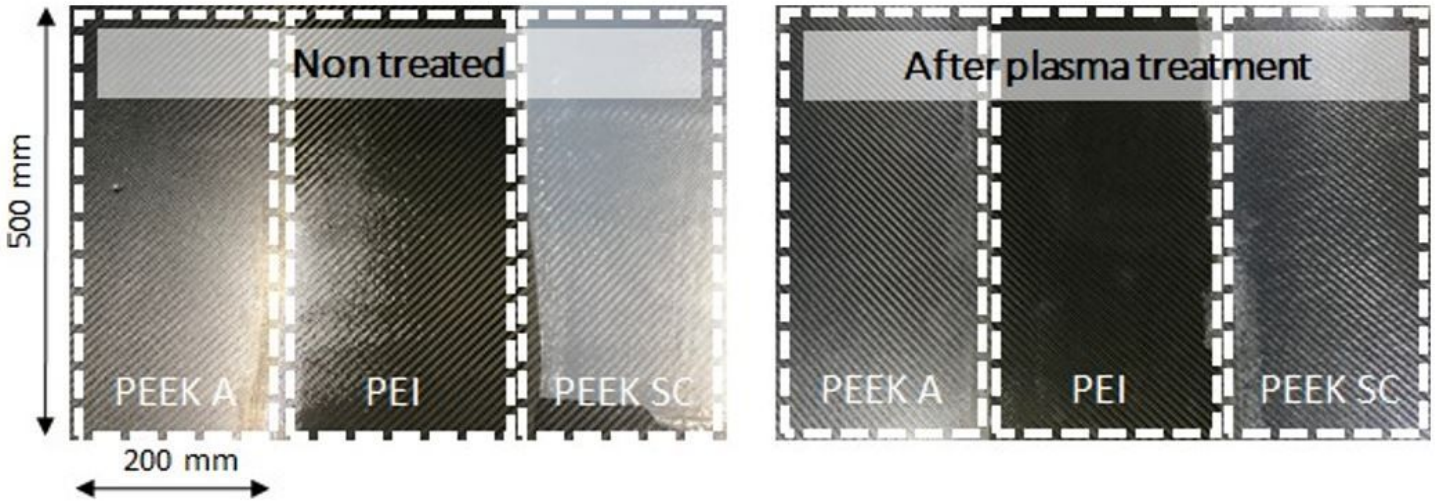

Figure 2

Functionalized TSC views after demoulding

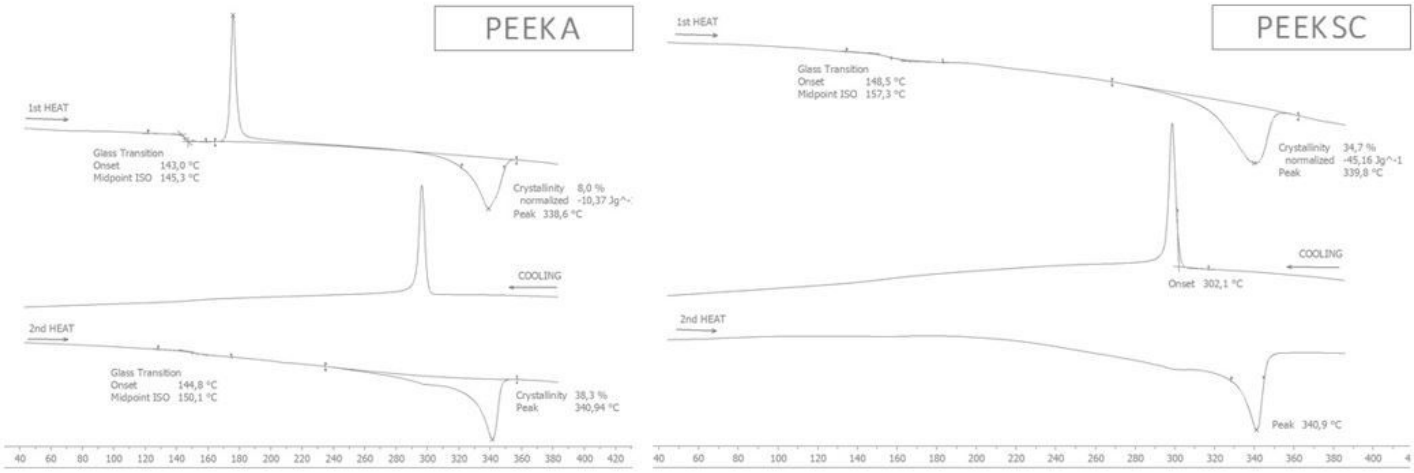

Figure 3

(A) View of the lower tool during the heat phase; (B) IR welding equipment ; (C) TPC/TSC welded plate

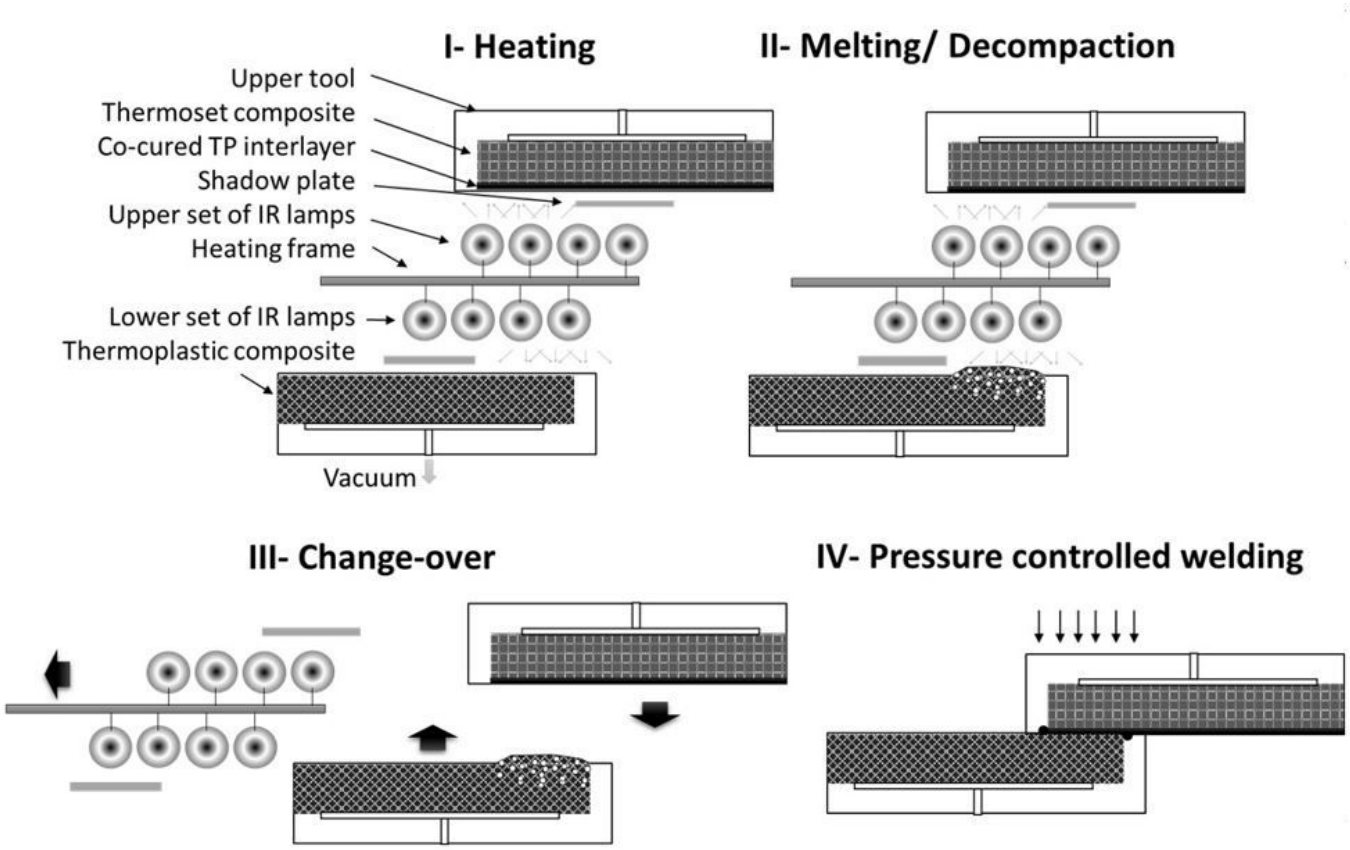

Figure 4

Infrared welding process description for TSC/TPC welding

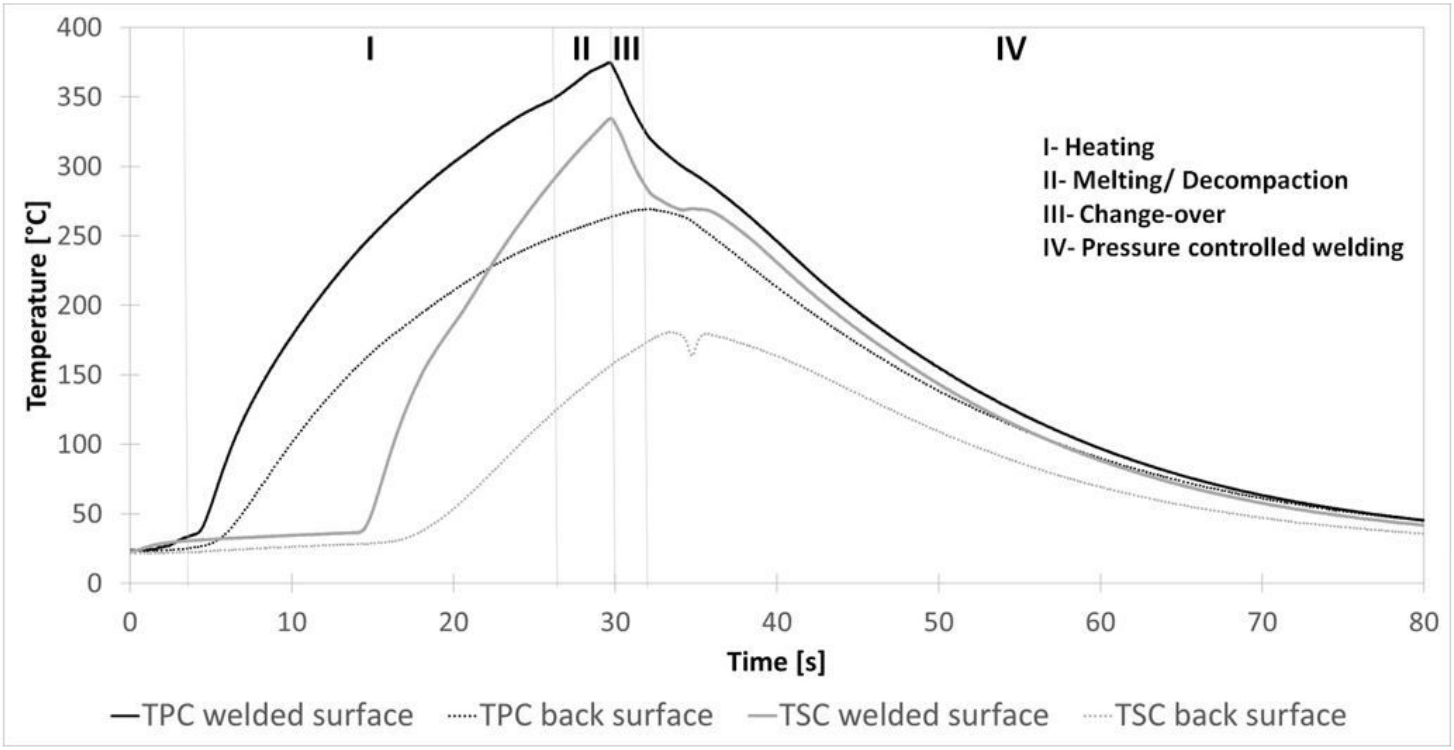

Figure 5

Measured temperature profiles during IR Welding

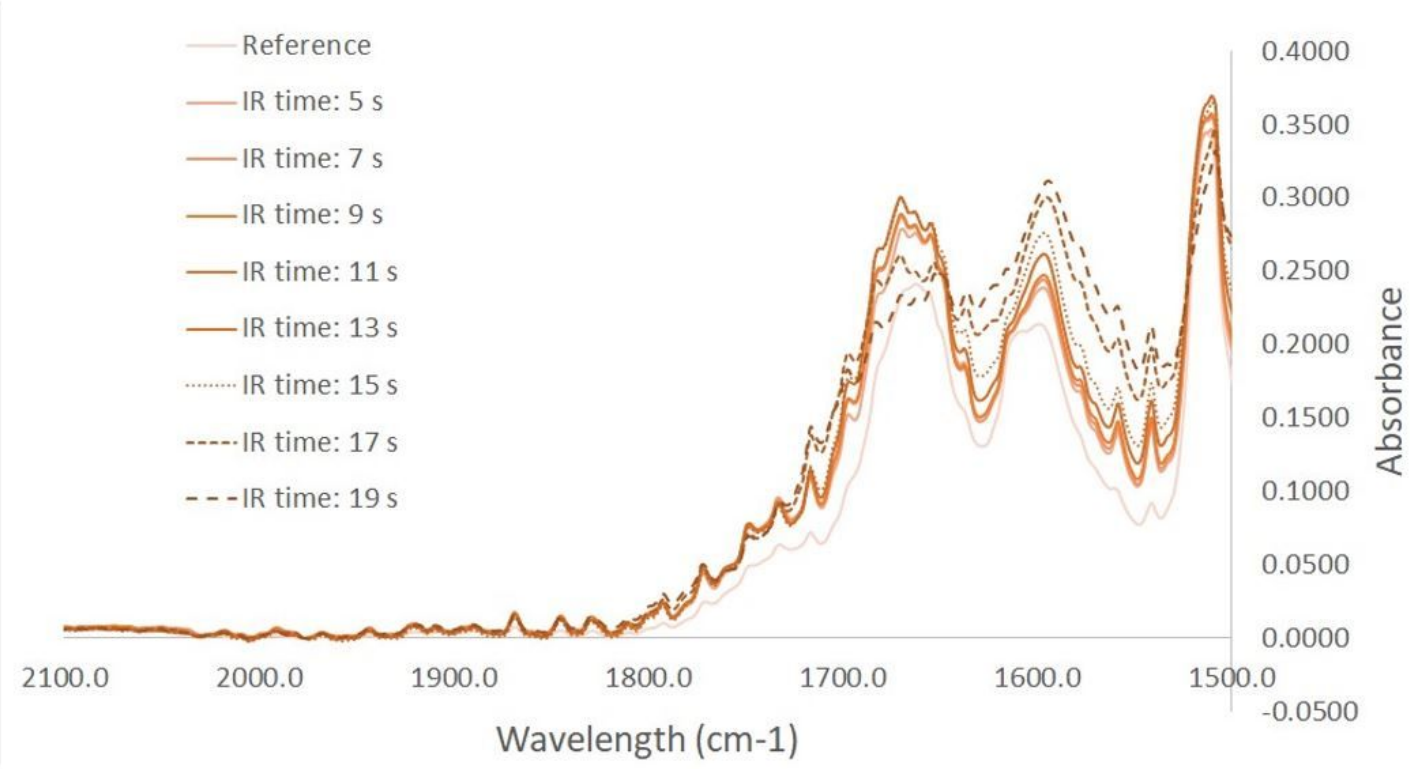

Figure 6

FTIR's normalized results for pure RTM6-2 as function of the Infrared time of exposure

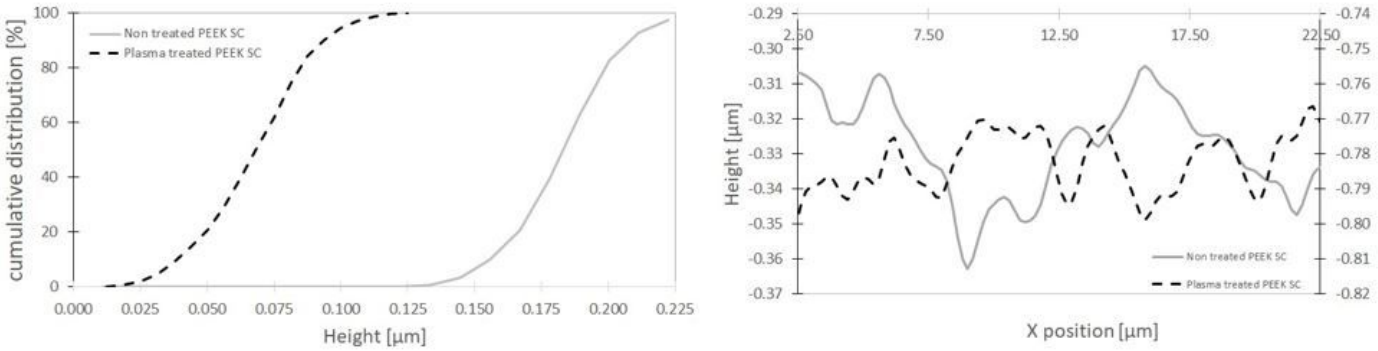

Figure 7

Roughness analysis of PEEK SC before and after plasma treatment: height distri- bution (right) ans roughness profile exemple (left)

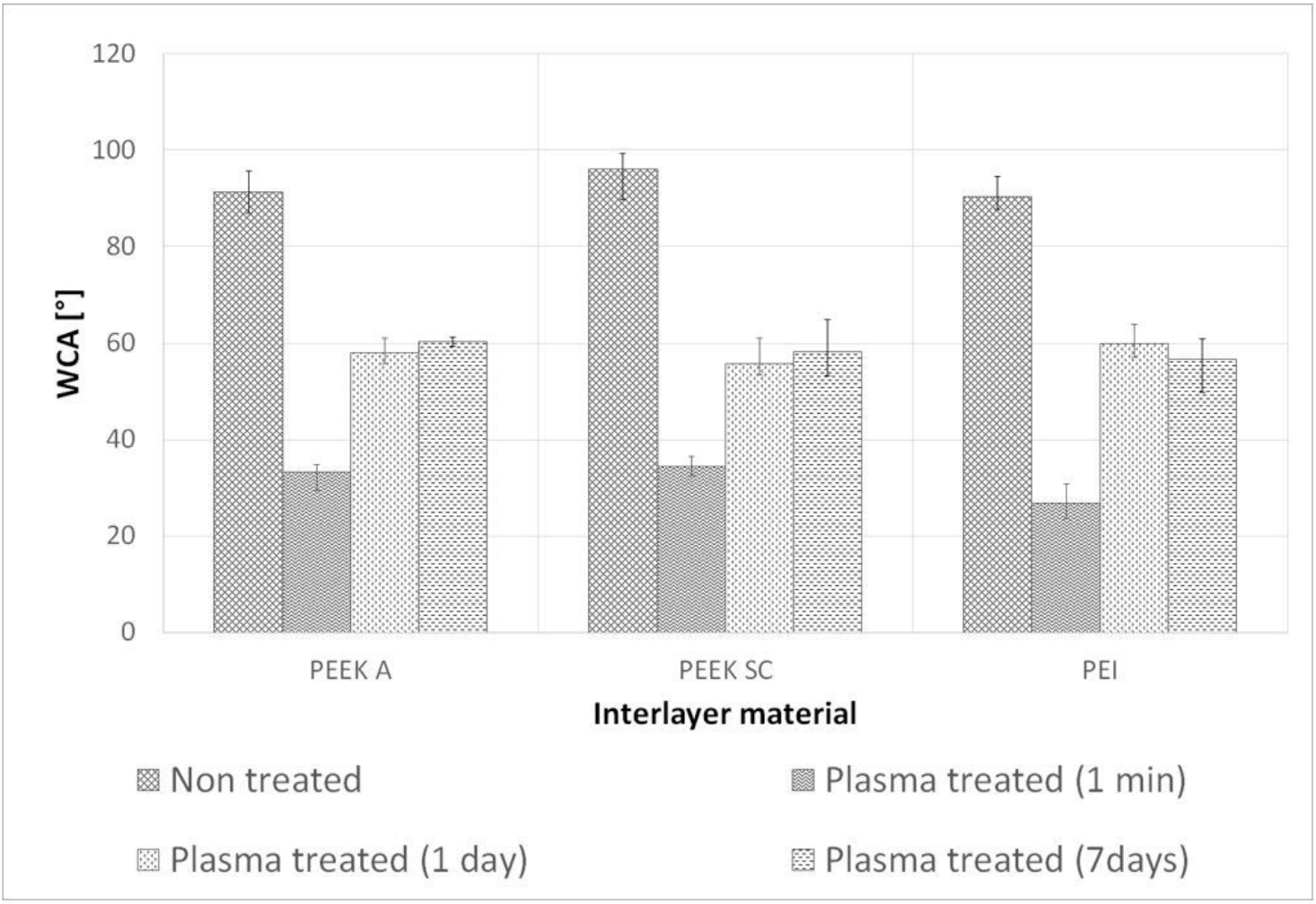

Figure 8

Wettability depending on waiting time after pasma treatment

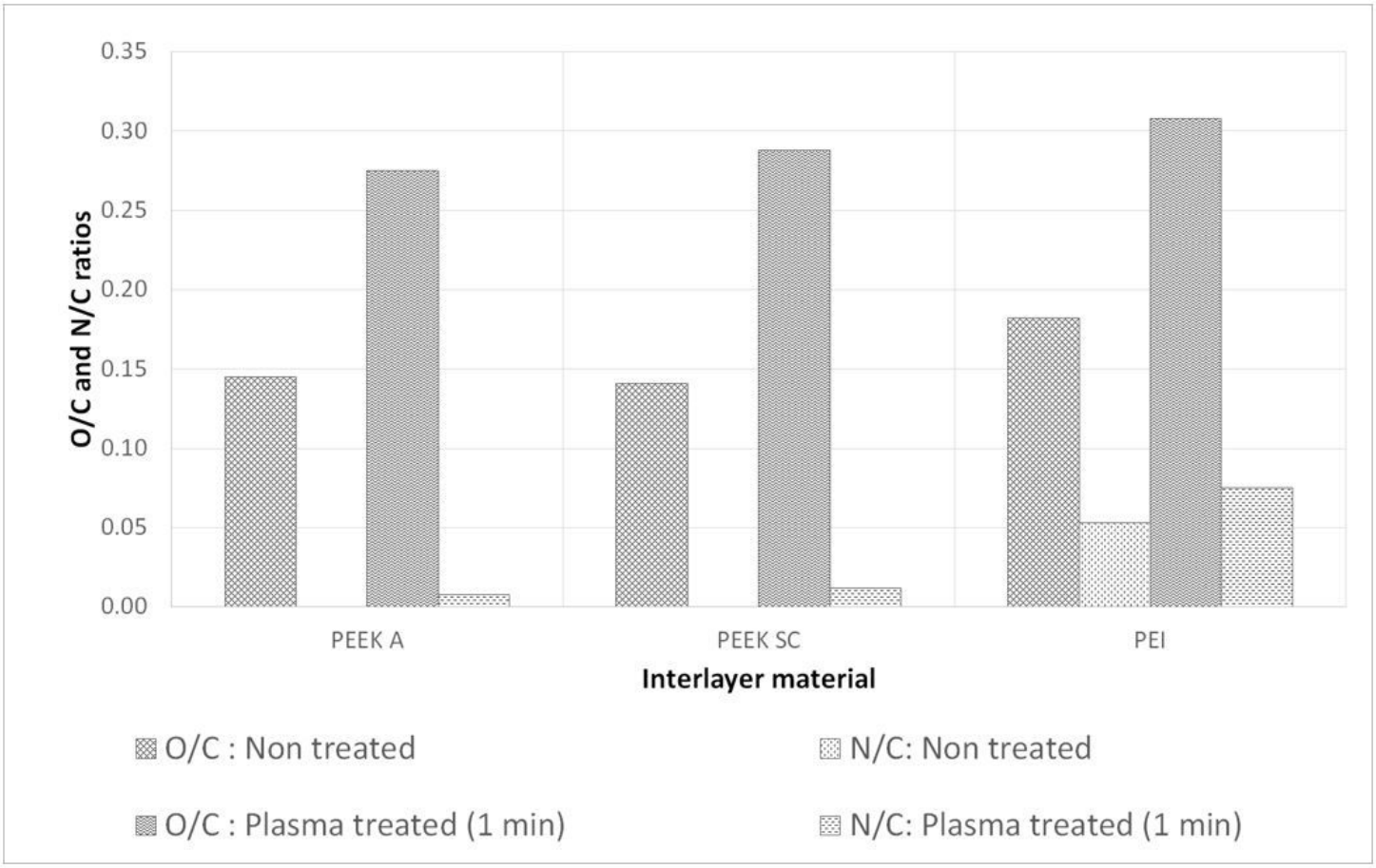

Figure 9

Investigation of O/C and N/C ratio by XPS

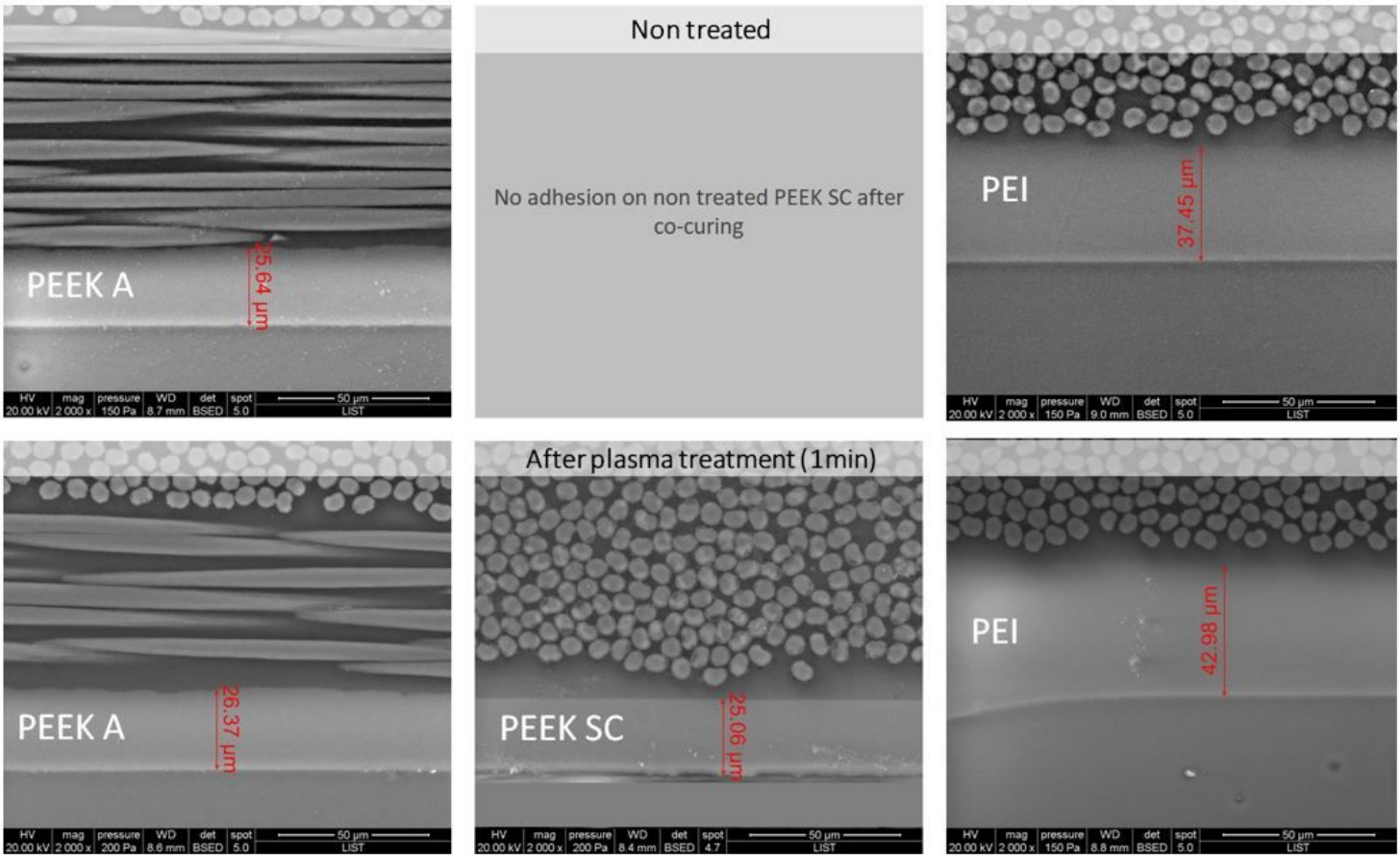

Figure 10

Cross section view by SEM of the functionalized TSC

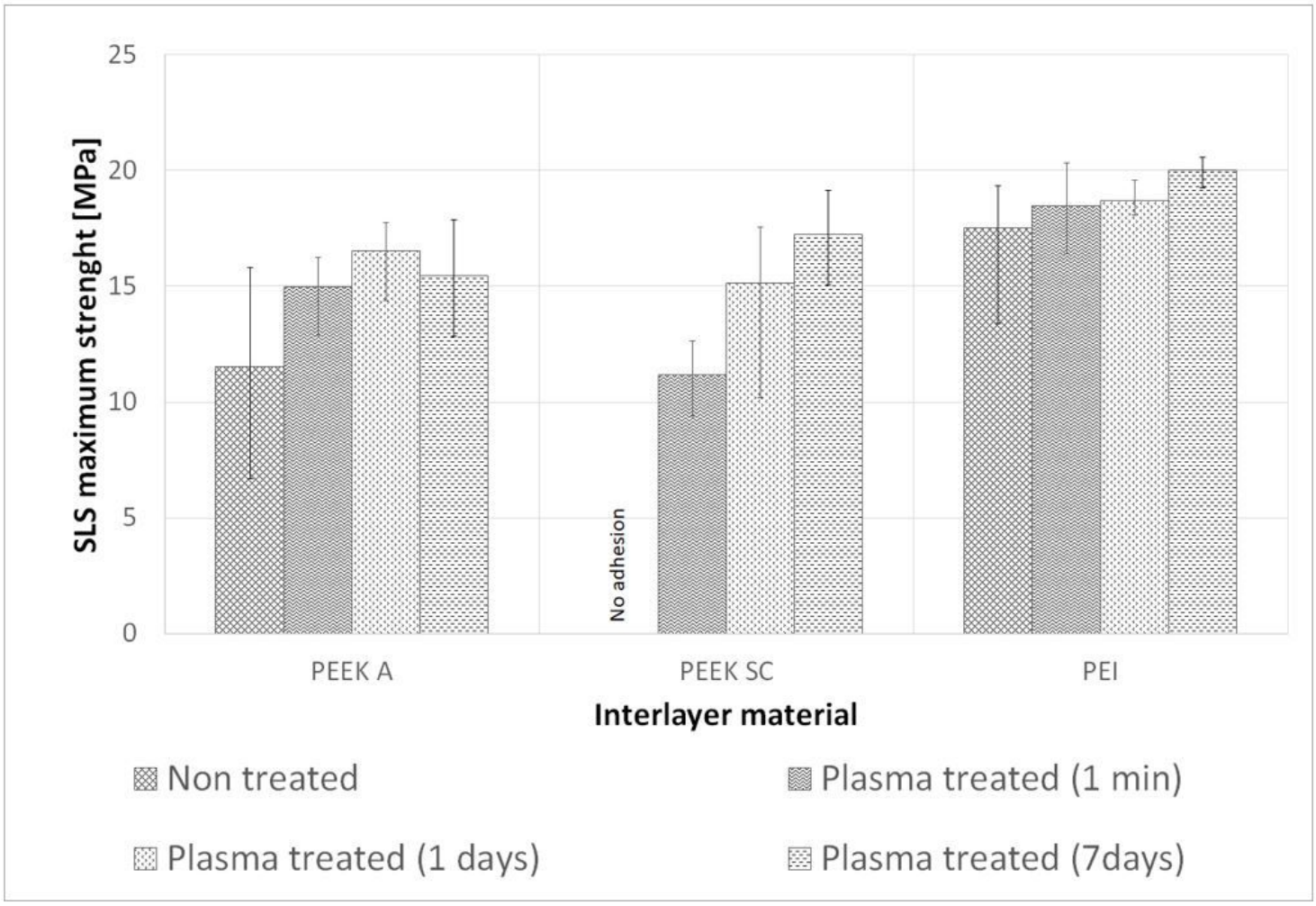

Figure 11

Single lap shear strentgh

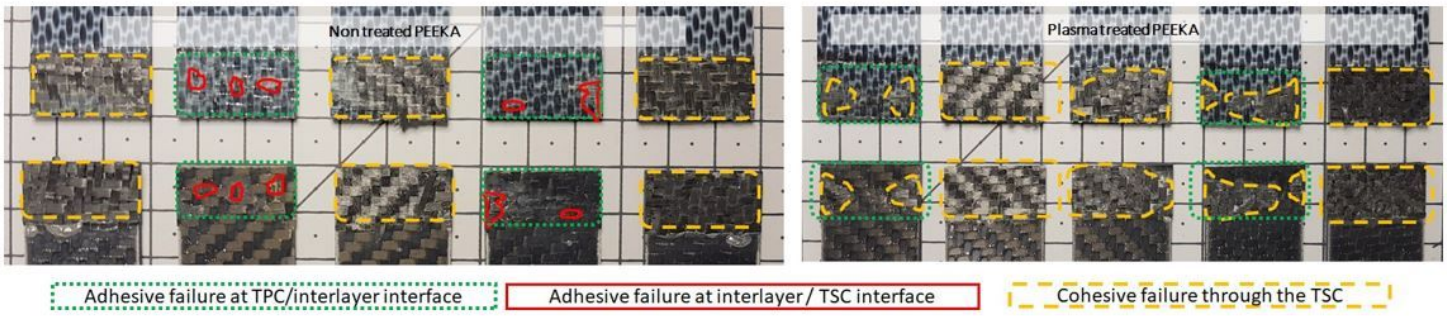

Figure 12

Failure mode analysis on non treatetd and plasma treated PEEK A interlayer's welded joins

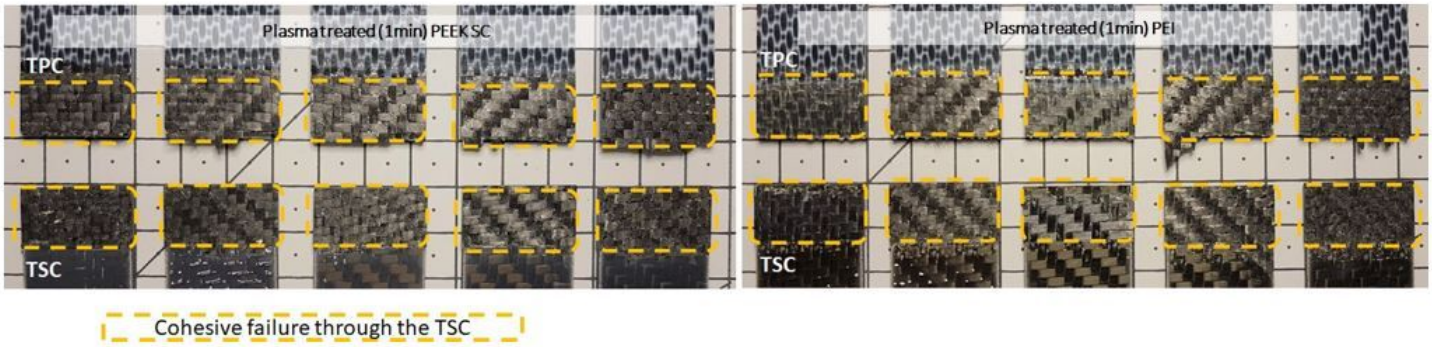

Figure 13

Failure mode analysis on plasma treated PEEK SC and PEI interlayer's welded joins